INVESTIGATION OF TUNGSTEN, COPPER, AND SILVER ALLOYS WITH INDIUM AT THE RAIL-ARMATURE INTERFACE ON A RAILGUN TEST BENCH

D. Gillich[1] and W. Maier[2]

[1] *United States Military Academy, Department of Physics, West Point, NY 10996*
[2] *Naval Postgraduate School, Physics Department, Monterey, CA 93940*

With the advent of electrically propelled ships, the Navy is now considering the use of electric power to launch projectiles in support of maritime land attack. Bore wear is one of the most significant challenges for a naval railgun program. The interface between the armature and rails is the most stressed point of a railgun because it transitions to liquid under high current densities. This liquid interface causes rail and projectile material to redistribute unevenly thereby produces rail degradation. Various combinations of tungsten, copper, and silver alloys were tested for rail and armature materials to determine which combination resulted in minimum damage during firing. The least degradation was observed with a silver-tungsten projectile and copper-tungsten rail: 10% loss in projectile mass for a current density of approximately 86 kA/cm^2. Indium at the interface protected the rails and projectile from damage at current densities under 21.5 kA/cm^2.

1 INTRODUCTION

One of the major challenges facing electromagnetic launch (EML) railguns is the degradation of the rail and armature during firing. This degradation is caused by uneven redistribution of material due to the liquid interface that forms at the rail-armature interface. In this paper we investigate the use of tungsten, copper, and silver alloys for rail and armature materials to determine which combinations result in minimum rail degradation.

We begin in Section 2 by providing the motivation for our work. We outline the apparent paradigm shift in the Navy's interest in the use of EML technologies as the basis for future weapon systems. In Section 3, we study the idea of using an interface material that will melt without damaging the rails or armature while acting as a "conductive lubricant" for the projectile.

A theoretical model is presented in Section 4 that allows us to determine the material parameters that are important for reducing rail degradation. Section 5 contains information about our experimental setup. We conclude Section 5 with a brief outline of the experiment. Experimentation was done in two phases: high current firing tests and low current density tests. In Section 6, we will present our procedure and experimental results for each of the two phases. Finally, concluding comments will appear in Section 7.

2 MOTIVATION: ARMY VERSUS NAVY APPLICATIONS

For two decades, the United States Army has conducted research in the field of EML railguns. The main focus has been on developing a "tank-killer" gun capable of defeating armor through direct-fire engagement with high-velocity projectiles (2-3 km/s). Within the past few years, the Army has further defined requirements to develop a launch platform that weighs less than 19,000 kg and is capable of being deployed in a C-130 aircraft. Given this new requirement, Army researchers are now focusing their efforts on developing more compact pulsed-power supplies and lighter yet stronger barrels [1].

In the past, the Navy's official position on the adoption of railgun technology has been to monitor the Army's railgun program. Recent developments, however, have increased interest in EML technology as the basis for future weapon systems. Currently, the Navy is considering EML technology for the mission of indirect fire in support of the littorals [2].

The origin of this paradigm shift in the Navy's focus is the Railgun Technology Assessment Report published by the Center for Naval Analysis (CNA) in 1998. In this report, reviewers determined that EML technology is sufficiently advanced to warrant further investigation for naval use. The CNA "recommends that the Navy pursue basic rail(gun) technology and provide modest funding to support a more detailed analytical study by the Navy's technical community, regarding the cost and effectiveness of railguns for maritime land attack"[2].

The Navy is also building electric propulsion ships with the advent of the destroyer, DD-21. In an electric ship, the EML railgun system can share its power supply with the electric propulsion system. This arrangement will save space and fuel as well as provide the opportunity to easily redirect tremendous amounts of energy [3].

The Navy's requirements for an EML railgun are different from the Army's. As mentioned earlier, the Army is developing a direct-fire system primarily designed for short, line-of-sight distances. The Navy, on the other hand, is interested in indirect firing engagements with extended range capabilities. Fig 1 gives an outline of the parameters that the Navy is considering for an EML railgun.

Range: 550 to 750 km (300 to 400 nmi)	Firing Rate: 6 rounds/min
Projectile Mass: 60 to70 kg	Power Use: ~ 60MW (at max range and rate)
Barrel Length: ≤ 15 m	Time of Flight: ~ 8 min (at max range)
Muzzle Velocity: 2.5 to 3.5 km/s	Cost: ≤ ~ $5K per round
Impact Velocity: 1.5 to 2.5 km/s	

FIGURE 1 Performance Parameters for a Notional Land Attack EM Gun [3].

3 RAIL-ARMATURE INTERFACE

The interface between the armature and the rails is a highly stressed location in an EM launcher: joule and frictional heating cause melting at the interface. This heating is associated with ablation on the rails or even gouging at hyper-velocities (velocities greater than 1.5 km/s) [4]. The change of the rail/armature interface to liquid is simply referred to as *transition.* "Reliable prevention of transition has proven difficult because no validated physical model of transition has been demonstrated" [5].

The Electromagnetic Armament System Focused Technology Program (EMAS FTP) has established exact parameters concerning the amount of ablation or bore growth (change). "The program requirement is a 0.4% of the bore diameter growth (change) over a 1000-shot life, which is equivalent to 0.2 μm of deposition per shot" [4]. The traditional combination of an aluminum projectile on copper rails yields about 25μm of deposition per shot, distributed unevenly on the rails.

When considering gouging at hyper-velocities, the effect of this liquid interface is not as easily understood. Researchers believe that a liquid interface may prevent or delay gouging at velocities over 1.5 km/s. However, the EML community lacks full understanding of the exact nature of the effects of a liquid armature-rail interface [4].

In the absence of a physical model to predict and prevent transition, researchers have adopted a trial-and-error approach to determine compatible rail and armature combinations. The central point to this type of approach is to determine what material parameters are relevant to the problem and to make an educated guess as to what combinations or materials are likely to yield successful results. Very likely, harder and more refractive materials will be less susceptible to melting and gouging.

As stated, the interface between the rail and armature changes to liquid under high current densities. The focus of the investigations being done at the Naval Postgraduate School in Monterey, California is to test different interface materials to reduce degradation of the rail or armature. By selecting materials that have low melting points, low vapor pressure, and high boiling points, we hope to find an interface material that will melt without damaging the rails or armature. This interface material must also act as a "conductive lubricant" for the projectile.

This idea is not entirely new. In 1972 a doctoral student at the Australian National University, J.P. Barber, dipped a copper projectile in lead-tin alloy (common solder) and fired the projectile with very little damage to the rails or base projectile. However, subsequent firing failed to reproduce the original results. As a suggestion for further research, Barber includes the use of "laminated projectiles dipped in a lower melting point material than solder (e.g. indium)" [6].

Another Australian, A.J. Bedford, conducted research in 1984 with different materials at the rail-armature interface. He tested copper rails (standard Cu-0.6%Cd alloy) that were plated with various materials and used a plasma armature (aluminum foil) to initiate firing. Bedford found that rails plated with zinc and tin gave promising results in terms of rail damage. He also concluded that "the behavior of Sn and Zn coatings in resisting deep arc damage, probably by melting and flowing, also suggests avenues for more investigation" [7].

4 THEORETICAL MODEL

When considering which materials are best to prevent degradation of the rail or armature, we must first determine what material properties pertaining to heat conduction are important. To get a rough estimate of these parameters, in what follows, we will ignore any conduction of heat due to friction.

The quantity of heat, dQ, required to change the temperature of a material of mass m an amount dT is given by

$$dQ = mcdT \tag{1}$$

where c is the specific heat of the material. When a quantity of heat dQ is transferred to a material in a time dt, the rate of heat flow, or power, is

$$P = \frac{dQ}{dt}. \tag{2}$$

Combining equations (1) and (2) we find that

$$P = mc\frac{dT}{dt}. \tag{3}$$

Now let us consider a small element of material with cross-sectional area A and length dx. We can express the mass of the material as

$$m = \rho A dx \tag{4}$$

where ρ is the mass density. If a current flows through the material, the electrical power dissipated is

$$P = I^2 R \tag{5}$$

where R is the resistance of the material. This resistance can be also be expressed in terms of a small element of length dx as

$$R = \frac{dx}{\sigma A}. \tag{6}$$

Here σ is the conductivity and A is the cross-sectional area through which the current flows. This allows us to combine equations (3)-(6) to obtain an expression for the current in terms of the material parameters, i.e.,

$$I^2 = \rho c \sigma A^2 \frac{dT}{dt}. \tag{7}$$

To get an idea of how these material parameters affect the momentum of the armature, we can obtain an expression for the current through the armature using the Lorentz force law, $F = \frac{1}{2}L'I^2$, and Newton's second law, $F = m\frac{dv}{dt}$. Doing so, we obtain

$$I^2 = \frac{2m}{L'}\frac{dv}{dt} \tag{8}$$

where L' is the inductance gradient. Combining equations (7) and (8) allows us to express the momentum, dp, of the armature in terms of material parameters

$$dp = mdv = \frac{\rho c \sigma A^2 L'}{2} dT . \tag{9}$$

To maximize the momentum we must maximize the right hand side of equation (9). For a rough approximation we will keep the specific heat, c, constant. Hence, the best materials for armature use are found through the material parameters $\rho c \sigma \Delta T$. Here we have replaced the infinitesimal temperature, dT, by ΔT. If we furthermore consider the mass of the armature to be constant we see that the material parameters which are important are the change in temperature of the armature, ΔT, and the conductivity, σ. The other variables that appear in equation (9) are parameters of the railgun geometry.

Tables 1 and 2 below give pertinent data concerning possible materials to be investigated. In Table 1, T_m is the melting temperature, T_b is the boiling temperature, and ΔT_m is the difference between room temperature (taken to be 20° C) and the melting temperature. We use ΔT_m for rail and armature materials because we do not want the rail or the armature to melt.

TABLE 1Rail/Armature Material Data [8]

Material	T_m (°C)	T_b (°C)	ρ (g/ml)	c (cal/g-°C)	σ (1/μΩ)	ΔT_m (°C)	ρcσΔT (cal/ml-μΩ)
Al	660	2450	2.7	0.215	0.382	640	142
Cu	1083	2595	8.96	0.092	0.593	1063	520
Mo	2610	5560	10.2	0.061	0.19	2590	306
Ag	960	2210	10.5	0.056	0.616	940	340
W	3410	5930	19.3	0.032	0.181	3390	379

In Table 2, T_m is the melting temperature, T_b is the boiling temperature, and ΔT_b is the difference between room temperature (taken to be 20° C) and the boiling temperature. We take this difference because we want the material at the interface to melt without boiling off. This will allow us to neglect any latent heat in our expression for equation (1).

Table 2 Interface Material Data [8]

Material	T_m (°C)	T_b (°C)	ρ (g/ml)	C (cal/g/°C)	σ (1/μΩ)	ΔT_b (°C)	ρcσΔT (cal/ml/μΩ)
Zn	419	906	7.14	0.091	0.167	886	96.1
Ga	30	2237	5.9	0.079	0.058	2217	52.4
In	156	2000	7.3	0.057	0.111	1980	78.5
Sn	232	2270	7.3	0.054	0.088	2250	68.3

5 BASIC EXPERIMENTAL COMPONENTS

5.1 Railgun Test Bench

A small test bench was constructed to test various materials at the rail-armature interface, Fig 2. The test bench was primarily made out of a phenolic with 4"-long by 1"-wide copper rail inserts. The test material is mounted on the end of the copper insert with screws as shown in Fig 3.

Given the dimensions of the railgun test bench, the inductance gradient is roughly estimated to be

$$L' = 8.9 \times 10^{-8} \left(\frac{henries}{meter} \right).$$

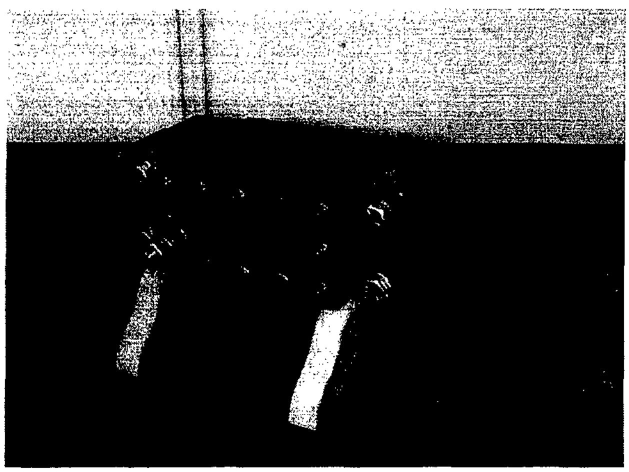

FIGURE 2 Railgun Test Bench

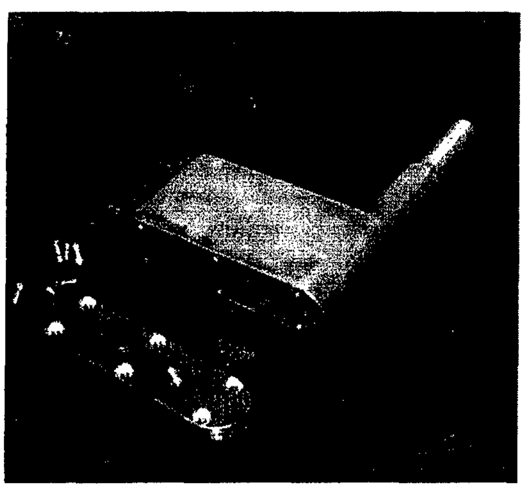

FIGURE 3 Copper Pole Piece with Test Rail Material

5.2 Power Unit

The power supply consists of two 830 μF capacitors rated at 10kV in parallel, two TVS-40 vacuum switches, and a diode crowbar circuit to prevent reverse charging of the capacitors. This pulse-power supply is capable of producing up to 200 kA of current and 80 kJ of energy [9]. To prevent failure in the crowbar circuit three strings of six DA24 F2003 high power avalanche diodes were installed. Proper installation of these diodes, manufactured by ABB Semiconductors AG of Lenzburg, Switzerland, require a mounting force of 20 kN at the center of the devices. Special mounting clamps were ordered from ABB Semiconductors and the three strings of diodes were installed, as seen in Fig 4. The internal inductance of the circuit was measured to be 2.4μH. We found that the period of this circuit is 0.4 ms and the resonant frequency of the circuit is 2.5 kHz.

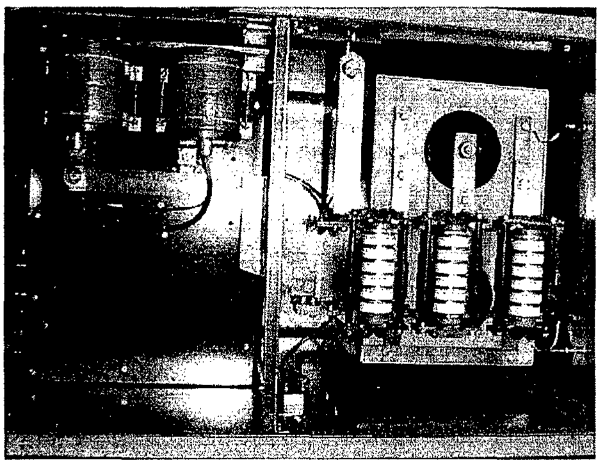

FIGURE 4 Power Unit

5.3 Projectile Design

The projectiles were designed to ensure constant contact between the rail surface and the armature. Two different designs were used. The first had a straight edge at the interface as shown in Fig 5. This provided a 0.6 cm^2 area at the interface. The 60° notch in the back of the projectile is designed to allow the projectile to expand when the Lorentz force drives the rails apart during firing.

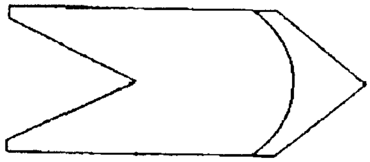

FIGURE 5 Solid Armature

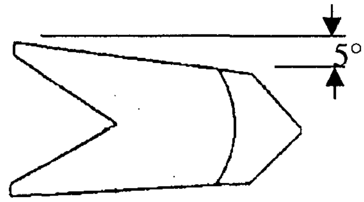

FIGURE 6 Hybrid Armature

The second type of armature is a hybrid armature, Fig 6. This design is fundamentally identical to the solid armature except for a 5° slope at the interface. The material in contact with the rails melts and turns into a conductive plasma, which may fill in the back of the projectile to provide the Lorentz force. Essentially, this design sacrifices the rear most portion of the projectile to melting while the bulk of the projectile remains undamaged.

Both types of armatures were used for high current density experiments while only the solid armature was used for low current density experiments. Table 3 provides the average projectile masses for the test materials before firing.

TABLE 3 Average Projectile Mass of Test Materials

Material	Average Mass
Al	0.81 g
Cu	2.50 g
CW 75	3.60 g
SW 50	4.60 g
Mo	3.43 g

5.4 Outline of the Experiment

Initial testing of materials using the railgun test bench was completed in two phases. Phase I was designed to stress the investigated materials with extremely high current densities. Under these conditions, the hope was to gain insight into which rail-armature material combinations are more suitable to use in the EML environment. These tests were also used to investigate the use of the test bench as a railgun by providing enough current to fire the projectile. During phase II the capacitor voltage was reduced, and materials were investigated at lower current densities. With these experiments, the value of the current at the point at which materials began to melt and/or move via the Lorentz force was determined.

The materials used for early firing tests were the traditional combination of bar stock copper rails with aluminum projectiles. After the railgun test bench fired successfully, other materials were tested. The primary materials used were copper-tungsten and silver-tungsten alloys for the armature and rails. The interface material was indium.

The data that was gathered during these tests is rudimentary. One of the shortcomings of this test bench is the lack of advanced diagnostics for gathering data.

6 EXPERIMENTAL PROCEDURES AND RESULTS

6.1 High Current Firing Tests

6.1.1 Procedure

The projectiles were started from rest approximately one inch from the end of the rail giving an effective rail length of three inches. The mass and size of the projectiles were measured before and after firing and the changes were calculated. The mass and the face-to-face width of the armatures were measured using a Mettler Macro-Balance, Model H 15 and a Mitutoyo Digimatic Caliper, 500 series, respectively. We also visually inspected the surfaces of the rails after each shot and recorded general observations. Additionally, some of the shots were video taped and photographed.

The current was measured using a Pearson wide band current monitor, Model 1330. To convert from the voltage reading received from the Hewlett Packard Infinium oscilloscope, Model HP 54845A, to determine the maximum current, I_{max}, the following formula was used

$$I_{\max} = \frac{(\max V)(92.58)}{0.005}(A) \tag{10}$$

where (max V) is the maximum voltage reading off the oscilloscope. We measured the correction factor for the two 20 dB attenuators to be 92.58. The term, 0.005, is the V/A conversion factor read off the data plate on the Pearson current monitor. We also used commercial computer simulation software, MicroSIM Eval8, to verify that the measured maximum voltage, (max V), and the calculated maximum current, I_{max}, were in agreement with the expected values. Fig 7 depicts a typical current output plot from the oscilloscope. A Shooting Chrony chronograph, Beta Model, was used to measure projectile velocity.

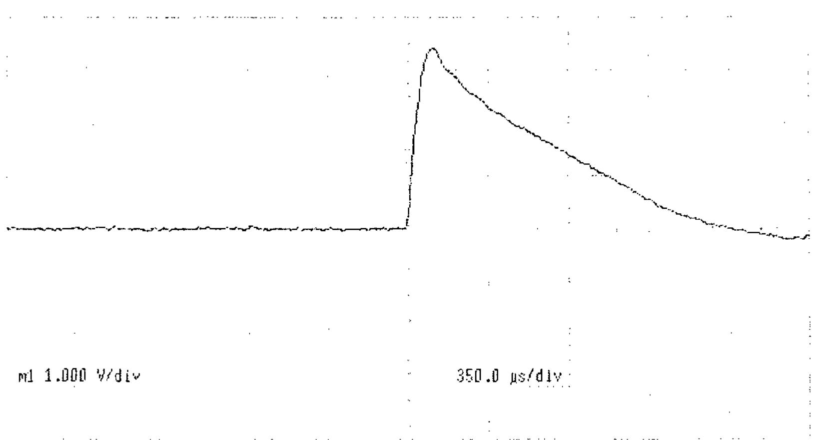

FIGURE 7 Oscilloscope Wave Form
(63 kA Current –Voltage Plotted on Ordinate Axis, Time Plotted on the Abscissa Axis).

6.1.2 Results and Discussion

Various combinations of rails and armatures were tested at different currents ranging from 48 kA to 67 kA. Table 4 summarizes the data collected for numerous shots.

Tests with aluminum armatures on copper rails yielded the predicted results. The copper rails were virtually undamaged but had a large amount of ablation from the projectile. The losses to the projectile in both mass and size were significant. Indium at the interface did not significantly change these results; in fact, for the tungsten alloy material combinations, a greater loss to the projectile was recorded.

Pure copper or aluminum armatures fired on silver-tungsten or copper-tungsten rails yielded worse results than aluminum on copper. The copper and aluminum broke down under Joule heating and extreme losses to the projectile in both size and mass were observed.

Table 4 Firing Test Data (S – Solid Projectile and H – Hybrid Projectile)

RAIL	Projectile (Solid/ Hybrid)	INTER FACE	V_0	I_{max}	% LOSS SIZE	% LOSS MASS	COMMENT
Cu	Al (S)	None	3 kV	No Reading	6 %	17.5%	Al Ablation on rails Chronograph-771 m/s
Cu	Al (S)	None	4 kV	51 kA	11%	21%	Al ablation on rails
Cu	Al (S)	None	4 kV	51 kA	14%	30%	Al ablation on rails
Cu	Al (S)	In	4 kV	51 kA	10%	25%	Al/In ablation
Cu	Al (S)	Al/In	4 kV	52 kA	21%	41%	Severe ablation on rails
Cu	Al (H)	None	4.5kV	56 kA	25%	32%	Severe ablation on rails
SW 65	Cu (H)	None	4 kV	52 kA	20%	24%	Minimal ablation on rails
SW 65	Cu (H)	In	4 kV	51 kA	22%	26%	Cu/In ablation on rails
SW 50	Al (S)	None	5 kV	63 kA	100%	100%	Projectile disintegrated - plasma out the bore
SW 50	Al (S)	None	4.5 kV	58 kA	25%	48%	Severe Al ablation on rails
SW 50	CW 75 (H)	None	5 kV	63 kA	15%	11%	Very little ablation on rails See Fig (4.7).
SW 50	CW 75 (H)	None	5 kV	66 kA	14%	17%	Very little ablation on rails
SW 50	CW 75 (H)	In	5 kV	63 kA	21%	19%	CW/In ablation on rails
CW 75	Cu (H)	In	5kV	62 kA	20%	26%	Chronograph-2894 m/s See Figure (4.6)
CW 75	SW 50 (H)	None	5 kV	62 kA	18%	19%	Half the projectile fractured
CW 75	SW 50 (H)	None	4 kV	52 kA	11%	10%	Rail gouge, little projectile ablation
CW 75	Mo (S)	None	4 kV	49 kA	7%	7%	Gouge on (-) and ablation on (+) rails

While firing a copper projectile on copper-tungsten rails with an indium interface, a chronograph reading of 2.9 km/s was obtained. We calculated the maximum feasible speed of the projectile given its mass and the energy in the system and determined that the projectile could not have traveled that fast. Upon reviewing videotape of the shot, we observed an indium/copper plasma spray traveling ahead of the projectile at a much greater speed. This spray triggered the chronograph, which was then unable to detect the velocity of the projectile itself.

Using combinations of the copper-tungsten and silver-tungsten yielded the most promising results given extremely high current densities. These projectiles were generally less ablated and had their original shape after exiting the railgun test bench, Fig 8. We concluded that the copper-tungsten, CW 75, melts before the silver-tungsten, SW 50. Again, projectile loses were slightly greater with the indium interface.

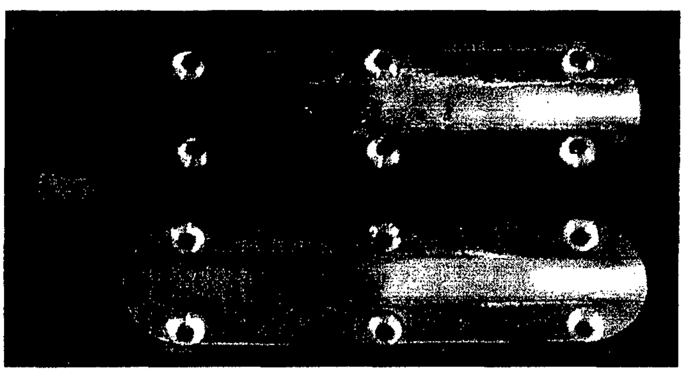

FIGURE 8 SW 50 Rails with CW 75 armature after a 63 kA shot.

The combination of SW 50 armature on CW 75 rails proved to be the most successful at high current densities using hybrid projectiles. With these shots, the projectile remained intact with material loss at the back of the hybrid projectile while the rail lost very little material through the breakdown of the CW 75. The material data for these materials is presented in Table 5.

TABLE 5 Copper/Silver-Tungsten Alloys Material Data

Copper-Tungsten Typical Properties				
Mi-Tech	Nominal Composition % Weight	Rockwell Hardness	Electrical Conductivity % IACS	Density GMS/CC
CW70	30 Copper- 70 Tungsten	90 B	50	14.18
CW75	25 Copper- 75 Tungsten	94 B	48	14.70
Silver-Tungsten Typical Properties				
SW50	50 Silver - 50 Tungsten	70B	65	13.4
SW65	35 Silver - 65 Tungsten	87B	53	14.5

Note: %IACS is International Annealed Copper Standard (i.e. %IACS of 50 means that CW70 has conductivity equal to 50% the conductivity of copper), Mi Tech Metals Inc. Indianapolis, IN

Finally, molybdenum projectile material on tungsten alloy rails must be investigated further. The amount of loss to the projectile is a promising result. However, the projectile velocity was noticeably slower since the projectiles fell short of the target sump in three shots. The low conductance of molybdenum may have caused this marked decrease in speed.

6.2 Low Current Density Tests

6.2.1 Procedure

After reviewing current literature discussing the parameters necessary for an operational naval railgun, we determined that the current densities imposed in phase I of this experiment were much higher than necessary.

A recently published paper by the Institute for Advanced Technology uses the parameter: "I'=I/h as a measure of linear current density on the inner surface of the rails that carry current (where h is the height of the rail at the inner bore from one insulator to the other)" [10]. In this paper, the authors give a conservative estimate for I'

$$I'=30\ (kA/mm) \tag{11}$$

Given this estimate and assuming h = 5" (127 mm) for a typical five-inch Naval gun,

$$I=3810\ (kA) \tag{12}$$

We further assume a 30 cm contact length between the projectile and rail to give a contact area of 381 cm^2. For a naval railgun the current density should then be about

$$\frac{I}{Area} = 10\left(\frac{kA}{cm^2}\right). \tag{13}$$

For the railgun test bench this current density, given the 0.6 cm^2 projectile contact area, yields a current of 6 kA, which equates to roughly a 250 V charge on the capacitors in our power supply.

To verify that equation (13) is a good assessment, we calculated another estimate from the Lorentz force equation and Newton's Second Law

$$\frac{1}{2}L'I^2 = ma \tag{14}$$

Here we assumed a 50 kg projectile and an average acceleration of 38.5 kilogees [10]. We calculated an estimate of the inductance gradient assuming, radius of 5 cm and a bore width of 12.7 cm. We get

$$L' = 5x10^{-7} \left(\frac{henries}{meter}\right) \tag{15}$$

Given the inductance gradient, the mass, and acceleration, we find the current, I, to be

$$I = 8.7x10^6 \text{ (A)} \tag{16}$$

Thus, given a contact area of 381 cm^2

$$\frac{I}{Area} = 23\left(\frac{kA}{cm^2}\right). \tag{17}$$

When comparing the two estimates above, equation (13) to equation (17), we find that the values are in agreement to within a factor of two.

During this phase of experimentation, the voltage of the capacitors was lowered, thereby reducing the current. Using the tungsten alloy materials, we determined at which voltage and current density the materials transitioned. Based on materials available and results found in phase I, we used CW 70 rails with SW 50 armatures. Solid armatures were used to ensure that there was a 0.6 cm^2 contact area with the rails. An indium interface between the same rail and armature combination was also investigated.

6.2.2 Results and Discussion

The projectile was placed in the bore to ensure a constant metal-to-metal contact between the armature and the rails, but was also able to accelerate when force was applied to it. We could then determine at what current densities the Lorentz force would initiate motion. Table 6 gives the results of this experiment.

The data suggests that the materials begin to break down at around 36 kA/cm^2. At 56 kA/cm^2, the projectile begins to accelerate under the Lorentz force before succumbing to joule heating and welding to the rails. A current density of 56 kA/cm^2 equates to roughly 34 kA given the railgun test bench parameters. This current density is roughly 5 times higher than necessary, given the estimate for naval railgun use in equation (13). At currents over 33 kA, the projectile appears to accelerate over a greater distances but also inflicts greater damage on the rails and armature.

We replicated the experiment with indium at the interface between the same combinations of materials. An electric hot plate was used to melt the indium. The melted indium was then applied to the contact face of the projectile by dipping the projectile into the liquid. As a result, an average of 0.127 grams and 0.0185 inches of indium was non-uniformly melted onto the projectiles. During each shot, plasma was ejected from the railgun test bench, however, the projectile failed to accelerate (except on one shot). Table 7 summarizes the results of subsequent firing test.

TABLE 6 SW50 Armature on CW 70 Rails

Voltage on Capacitor (V)	Current Density (kA/cm^2)	Results
500	10	No change in projectile or rail.
1000	22	No change in projectile or rail.
1600	36	Small contact-spot (0.012" diameter) on armature and rail.
2000	44	Armature welded to a 0.094" diameter. Weld spot is 0.17" from the back of projectile.
2500	56	Armature appears to have moved 0.36" before welding to a 0.129" diameter. Weld spot is 0.17" from the end of the projectile.
2500	54	Armature appears to have moved 0.04" before welding to a 0.4" diameter. Weld spot appears across the contact area of the projectile.
3000	64	0.52" movement. Welded to a diameter of 0.15". Weld spot is 0.17" from the back of the projectile.

The results here are promising. Comparing these results to those in Table 6, we see a significant reduction in loss to the projectile. Indium evidently protects the rails and projectile from damage at lower current densities.

TABLE 7 SW 50 Armature on CW 70 Rails with Indium Interface

Voltage on Capacitor (V)	Current (kA)	Loss in size	Loss in mass	Results
500	5	No data	No data	No damage to rail/projectile except for indium loss
1000	12	10%	4%	No damage to rail/projectile. Indium completely gone off projectile.
1000	13	1%	1%	No damage to rail/projectile. Some indium left on the projectile.
1000	13	3%	2%	Welded to (-) rail. No damage to (+) rail and after extraction little damage to (-) rail. Projectile has some indium left.
1250	15	7%	1%	Small amount of pitting on rails. Indium gone off the projectile.
1500	18	4%	2%	More severe pitting on rails. 0.66" movement of projectile. Indium gone off the projectile.
2000	26	5%	2%	More severe damage to rails. Projectile slightly damaged, indium gone.

Comparison of data in Table 6 and Table 7 also implies that the tungsten alloy materials melt at lower currents with the indium interface than without it. The Lorentz force appears to accelerate droplets of liquid indium faster than the projectile. Arcing between the projectile and the rails after the indium interface has left the bore may cause rail and armature materials to melt at lower currents. This effect would also explain the slightly higher percentage of losses, seen in Table 4, with an indium interface at higher current densities.

A maximum current of 13 kA, which equates to a current density of 21.5 kA/cm^2, is apparently where the rail/projectile material begins to break down. Again, this current density is up to 2 times greater than what is apparently necessary for naval railgun use. A projectile must be designed to keep the indium interface from blowing by the projectile before the Lorentz force is able act.

7 CONCLUDING COMMENTS

Initial testing of materials on a railgun test bench yielded promising results. Tungsten alloys were tested for the rail and armature materials; with a SW50 (50% W - 50% Ag) projectile and CW75 (75% W - 25% Cu) rail combination yielding the best results in our tests. Indium at the interface does protect the rails and projectile from damage at lower current densities. The projectile design must be improved. Indium may need to be better integrated into the projectile. This may allow the Lorentz force to act upon the projectile as a whole before the interface material blows past the projectile.

An investigation into different alloys at the interface may also prove to be beneficial. Materials that have an extensive plastic range may be more advantageous than the pure indium used here. Completely different interface materials also need to be investigated. Table 2 provides a list of possible materials.

ACKNOWLEDGMENTS

This paper is adapted from a Masters Thesis written by D. Gillich [11]. We are grateful for the support received from the Naval Postgraduate School on this work. We extend our deepest gratitude to Don Snyder, George Jaksha, and Gary Beck. Without their ingenuity and dedication this work would not have been possible. We'd also like to thank LT Mark Adamy for his assistance in the lab and his continuing work with the railgun project at NPS. Keith Aliberti is also gratefully acknowledged for his careful reading of the manuscript and his many useful comments.

REFERENCES

1. Ogorkiewicz, R.M., *In Search of Lighter, Smaller Electric Guns for Future Tanks,* Jane's International Defense Review, Vol. 032, Issue: 001, pp. 1-6, 1999.
2. Center for Naval Analysis Report CRM 98-74, *Railgun Technology Assessment,* by Kohlberg, I. and Bomse, pp. 3-15, 1998
3. Luke, I.T. and Stumborg, M.F., *The Operational Value of Long Range Land Attack EM Guns to Future Naval Forces,* submitted for publication to IEEE Transactions on Magnetics, pp. 1-4, 1999
4. Persad, C., Yoh, A., Prabhu, G., White, G., and Eliezer, Z., *On the Nature of the Armature-Rail Interface: Liquid Metal Effects,* IEEE Transactions on Magnetics, Vol. 33, No. 1, pp. 1140-145, 1997
5. Persad, C., *Solid Armature Performance: A Progress Report 1980-1990,* IEEE Transactions on Magnetics, Vol. 33, No. 1, pp. 134-139, 1997
6. Barber, J.P., *The Acceleration of Macroparticles and a Hypervelocity Electromagnetic Accelerator,* Doctoral Dissertation, The Australian National University, Canberra, A.C.T., March 1972
7. Bedford, A.J., *Rail Damage and Armature Parameters for Different Railgun Rail Materials,* IEEE Transactions on Magnetics, Vol. MAG-20, No. 2, pp. 352-355, 1984
8. Table of Periodic Properties of the Elements, Sargent-Welch Scientific Company, 1968
9. Lockwood, M., *Design and Construction of an Expandable Series Trans-Augmented Electromagnetic Railgun,* Master's Thesis, Naval Postgraduate School, Monterey, California, June 1999
10. McNab, I.R., Fish, S., and Stefani, F., *Parameters for an electromagnetic Naval Railgun,* Institute for Advanced Technology, The University of Texas at Austin, IAT.P 0367, pp. 1-6, 1999
11. Gillich, D., *Design, Construction, and Operation of an Electromagnetic Railgun Test Bench,* Master's Thesis, Naval Postgraduate School, Monterey, California, June 2000